JOURNAL OF GEOPHYSICAL RESEARCH, VOL. 104, NO. C9, PAGES 20,551–20,570, SEPTEMBER 15, 1999

The role of the Indonesian Throughflow in equatorial Pacific thermocline ventilation

Keith B. Rodgers,[1] Mark A. Cane, and Naomi H. Naik

Lamont-Doherty Earth Observatory, Columbia University, Palisades, New York

Daniel P. Schrag

Department of Earth and Planetary Sciences, Harvard University, Cambridge, Massachusetts

Abstract. The role of the Indonesian Throughflow (ITF) in the thermocline circulation of the low-latitude Pacific Ocean is explored using a high-resolution primitive equation ocean circulation model. Seasonally forced runs for a domain with an open Indonesian passage are compared with seasonally forced runs for a closed Pacific domain. Three cases are considered: one with no throughflow, one with 10 Sv of imposed ITF transport, and one with 20 Sv of ITF transport. Two idealized tracers, one that tags northern component subtropical water and another that tags southern component subtropical water, are used to diagnose the mixing ratio of northern and southern component waters in the equatorial thermocline. It is found that the mixing ratio of north/south component waters in the equatorial thermocline is highly sensitive to whether the model accounts for an ITF. Without an ITF, the source of equatorial undercurrent water is primarily of North Pacific origin, with the ratio of northern to southern component water being approximately 2.75 to 1. The ratio of northern to southern component water in the Equatorial Undercurrent with 10 Sv of ITF is approximately 1.4 to 1, and the ratio with 20 Sv of imposed ITF is 1 to 1.25. Estimates from data suggest a mean mixing ratio of northern to southern component water of less than 1 to 1. Assuming that the mixing ratio changes approximately linearly as the ITF transport varies between 10 and 20 Sv, an approximate balance between northern and southern component water is reached when the ITF transport is approximately 16 Sv. It is also shown that for the isopycnal surfaces within the core of the equatorial undercurrent, a 2°C temperature front exists across the equator in the western equatorial Pacific, beneath the warm pool. The implications of the model results and the temperature data for the heat budget of the equatorial Pacific are considered.

1. Introduction

A series of model runs have been conducted to look at the role of the Indonesian Throughflow (ITF) in the thermocline circulation of the equatorial Pacific Ocean. The ITF refers to the mean export of waters from the western equatorial Pacific to the Indian Ocean via the Indonesian Straits separating the Australian and Asian continents. The role of the ITF in the global thermohaline circulation has been discussed by *Gordon* [1986], and its impact on global circulation and thermal budgets has since been addressed in several modeling studies [*Hirst and Godfrey*, 1993; *Shriver and Hurlburt*, 1997]. Our investigation differs from previous studies in that we focus specifically on how the ITF affects circulation fields and thermal budgets within the pycnocline of the equatorial Pacific Ocean.

Our goal is to develop a better quantitative understanding of the sources of the water that upwells in the equatorial Pacific. We seek to identify not only the range of density surfaces that contributes to the equatorial upwelling but also the relative contributions of Northern and Southern Hemispheric component water that upwells along the equator. In ocean circulation models that treat the Pacific Ocean as a closed basin (thereby ignoring the transport of the ITF), equatorial upwelling is primarily supplied by water from the Northern Hemisphere subtropics. This is inconsistent with salinity measurements in the equatorial thermocline [*Tsuchiya et al.*, 1989], which suggest that the Southern Hemispheric component of the equatorial undercurrent is larger than the Northern Hemispheric component. One of our primary objectives is to quan-

[1]Now at Max-Planck-Institut für Meteorologie, Hamburg, Germany

Paper number 1998JC900094.
0148-0227/99/1998JC900094$09.00

tify the model sensitivity of the mixing ratio of northern to southern component thermocline water in the equatorial upwelling to the opening and closing of the Indonesian Straits. This has implications for climate variability because isopycnal surfaces from northern and southern sources have different temperatures.

This exercise is motivated by two broader scientific questions: What dynamical processes determine the mean thermal structure of the pycnocline in the equatorial Pacific? What dynamical processes control the time variability of the thermal structure of the pycnocline? Modeling studies have shown that changes in the thermal structure of the equatorial thermocline can change the decadal variability of the El Niño-Southern Oscillation (ENSO). In fact, of all the parameter sensitivity studies that have been conducted with the coupled *Zebiak and Cane* [1991] model, changing the temperature structure of the thermocline has the strongest influence on model behavior.

To first order, in a zonally averaged sense, a subtropical cell (STC) [*McCreary and Lu*, 1994], exists in the upper thermocline of the Pacific Ocean, whereby much of the water that upwells along the equator has subducted in the subtropical gyres of the South and North Pacific. The upwelled water returns to the subducting regions of the subtropics through the surface Ekman flow. Temporal variability in the thermal structure of the equatorial pycnocline (below the euphotic zone) on isopycnal surfaces is described by the advection-diffusion equation for temperature anomalies

$$\frac{\partial T'}{\partial t} + \overline{\mathbf{u}}\cdot\nabla T' + \mathbf{u}'\cdot\nabla\overline{T} = K + K' \qquad (1)$$

where K represents isopycnal mixing and K' represents diapycnal mixing. The terms $\overline{\mathbf{u}}$ and $\overline{T}$ represent the time mean three-dimensional velocity and temperature fields, respectively, and $\mathbf{u}'$ and T' represent perturbations to the time mean fields. We have assumed that temperature anomalies can be treated as passive tracers, and we have ignored the perturbation product term. The second term on the left-hand side of (1) represents the advection of temperature anomalies by the mean flow, and the third term on the left-hand side represents changes associated with anomalous currents acting on the time mean temperature gradients along isopycnals in the equatorial pycnocline.

Recently a mechanism was proposed by *Deser et al.* [1996], *Gu and Philander* [1997], and *Zhang et al.* [1998], whereby temperature anomalies of order 0.5°C originating at the sea surface in the subtropics can advect subsurface into the equatorial thermocline via the STC and thus change the thermal structure of the equatorial pycnocline. It was suggested that it is the advective timescale of intergyre exchange between the subtropical subducting regions and the equatorial upwelling that determines the period for decadal-scale climate variations. The proposed mechanism assumes that advection associated with perturbation velocities acting on the mean background temperature gradients is not important. It also assumes low diffusivity and velocity shear within the thermocline, so that the extratropical anomalies are relatively intact upon reaching the equator. This amounts to assuming that the STC is a closed system, where the changes in temperature on isopycnal surfaces are described by

$$\frac{\partial T'}{\partial t} \approx -\overline{\mathbf{u}}\cdot\nabla T' \qquad (2)$$

However, the low prebomb Δ^{14}C values recorded by Galapagos (1°S, 90°W) corals [*Druffel*, 1981, 1987] suggest that the STC is not a closed system, in that significant amounts of water from below the equatorial pycnocline are entrained into the equatorial upwelling [*Toggweiler et al.*, 1991]. The term $\mathbf{u}'$, which includes changes in upwelling velocities, is known to be significant in the equatorial Pacific. In addition, the equatorial $\nabla\overline{T}$, which includes the time mean temperature gradient along the isopycnal surface corresponding to the core of the equatorial undercurrent, is significantly larger than the $\nabla T'$ term emphasized by *Deser et al.* [1996].

In this paper we investigate the sensitivity of the circulation within the equatorial thermocline to the transport of the ITF. First, we present an overview of estimates of throughflow transport. This is followed by a presentation of our modeling results. We finish with a discussion of thermal budgets within the equatorial Pacific thermocline, where we refer to temperature and salinity measurements within the equatorial thermocline.

2. Observations

2.1. Thermocline Circulation for the Western Pacific

The mean flow configuration within the thermocline of the low-latitude western Pacific is shown schematically in Figure 1. The focus is on flow within the pycnocline, which corresponds to the potential density range σ_θ=25.0 to 25.5 and which lies at a mean depth of between 150 and 200 m in this region. This is the density range feeding the core of the Equatorial Undercurrent (EUC) in the western Pacific.

The South Equatorial Current (SEC) and the North Equatorial Current (NEC) represent the westward flowing, equatorward branches of the southern and northern subtropical gyres, respectively. The Mindanao Current and the New Guinea Coastal Undercurrent (NGCUC) are both low-latitude western boundary currents, which transport high-salinity subtropical thermocline water into the equatorial region. Much of the high-salinity southern component water has reached 143°E via the Vitiaz Strait, stretching between Papua New Guinea and New Britain at approximately 6°S, 148°E (see Figure 1). *Murray et al.* [1995] measured a transport through the Vitiaz Strait of approximately 15 Sv in

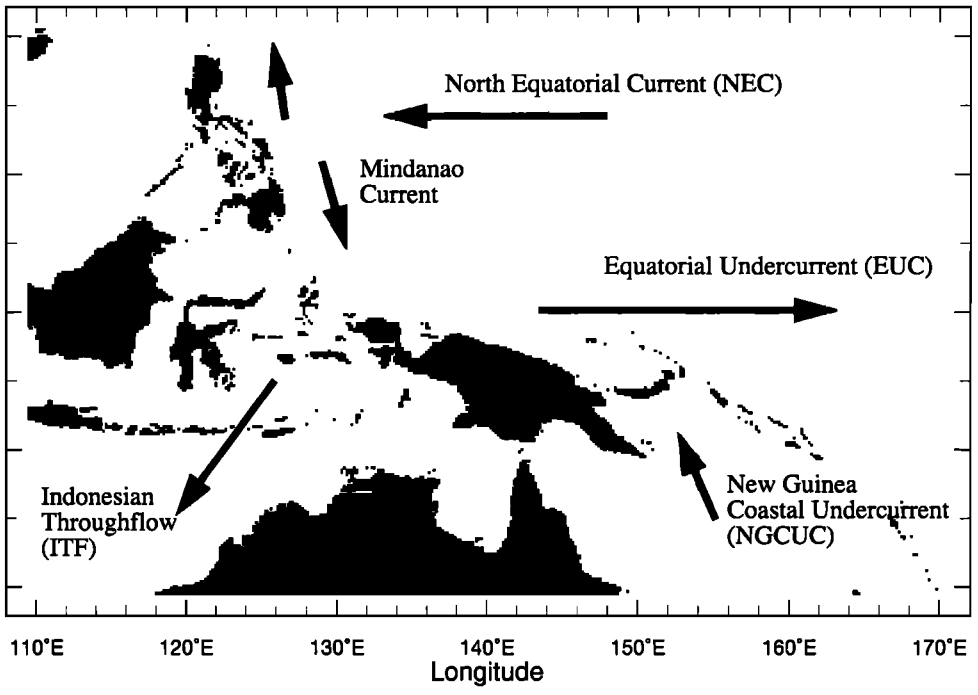

Figure 1. Schematic representation of thermocline flow in the western equatorial Pacific Ocean.

1992. The magnitude of this transport is quite large, especially when considering that the channel through which it flows is only 50 km wide and 1 km deep.

2.2. Hydrography of the Pacific Thermocline

There is a meridional salinity gradient along isopycnals across the equatorial thermocline of the Pacific Ocean that results from differences in freshwater fluxes at the sea surface between the North Pacific and the South Pacific. As a consequence, isopycnals in the Pacific thermocline are warmer and saltier in the South Pacific than they are in the North Pacific. This can be seen in Figure 2, which shows the salinity distribution on the σ_θ=25.0 isopycnal surface, where *Levitus et al.* [1994] annual mean salinity data have been linearly interpolated onto the σ_θ=25.0 surface calculated using both the annual mean temperature [*Levitus and Boyer*, 1994] and salinity climatologies. This density surface was chosen because it corresponds to the density of the EUC core. The freshest waters can be seen within the California Current in the northeastern part of the plot, advecting southward within the thermocline. The saltiest waters are found in the subtropical gyre of the South Pacific.

Wyrtki [1981] used thermal budgets to argue that the mean upwelling flux in the equatorial Pacific is 50 Sv. Both tritium (^{3}H) to helium 3 (^{3}He) ratios [*Jenkins*, 1996] and chlorofluorocarbons [*Warner et al.*, 1996] reveal a 10-20 year ventilation age for the core of the equatorial undercurrent. *Tsuchiya et al.* [1989] used measurements of the meridional salinity gradient collected during the Western Equatorial Pacific Ocean Circulation Study (WEPOCS) II survey along 143°E to argue that 1/2 to 2/3 of the water feeding the equatorial undercurrent in the western Pacific is supplied from the South Pacific. The WEPOCS II section at 143°E is near the confluence of the Mindanao Current and the NGCUC, and thus salinity measurements collected on the equator at this longitude can be used to infer the relative mixing ratio of northern subtropical component water to southern subtropical component water within the Equatorial Undercurrent. Since, as discussed below, interannual variability in temperature and salinity along isopycnal surfaces in this region is substantial, one should exercise caution in interpreting mixing ratios from one survey.

2.3. Indonesian Throughflow and Its Connection to Pacific Circulation

The thermocline circulation in the western equatorial Pacific is complicated by the presence of the Indonesian Throughflow. *Ffield and Gordon* [1992] have demonstrated using hydrographic measurements that the source of the ITF is North Pacific thermocline water. This North Pacific water mass is supplied to the ITF by the Mindanao Current. Given that the mean ITF transport (O(10 Sv)) is an order of magnitude larger than flow through the Bering Strait (O(1 Sv)), mass conservation requires that the ITF transport be compensated by cross-equatorial flow from the Southern Hemisphere. Thus although the NGCUC supplies perhaps 15 Sv to the equatorial pycnocline from the Southern Hemisphere, it does not itself close the flow around Australia by directly feeding the ITF. Rather, it

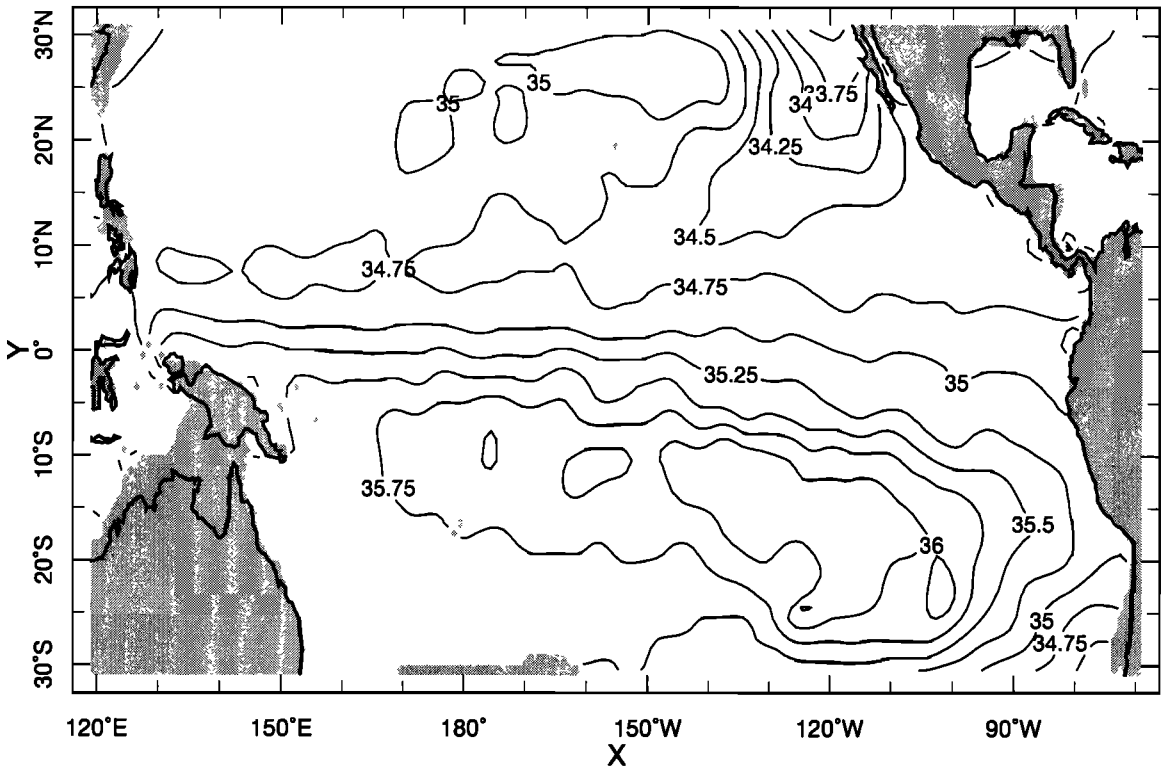

Figure 2. The salinity on the σ_θ=25.0 isopycnal surface, calculated from the *Levitus et al.* [1994] and *Levitus and Boyer* [1994] annual mean climatologies.

retroflects near 140°E in the Halmahera eddy and feeds the EUC. Upon upwelling in the eastern equatorial Pacific, some of this water is advected within the surface Ekman flow into the Northern Hemisphere. Through its exposure to surface fluxes, it undergoes a water mass transformation, before eventually subducting as northern component thermocline water.

Many attempts have been made to estimate the transport of the ITF using hydrographic data. An overview of recent estimates has been presented by Godfrey [1996], and they range from -2.6 Sv [*Fieux et al.*, 1996] to 18.6 Sv [*Fieux et al.*, 1994]. However, there are many complications involved with this method. The strong tidal mixing within the straits makes geostrophic calculations of doubtful validity.

Another approach to estimating the transport of the throughflow, *Godfrey*'s [1989] Island Rule calculates the mean transport of the ITF from the annual mean wind stress τ over the surface ocean. It makes a few approximations regarding the dynamical equations governing the mean flow in the ocean interior, including the assumption that the throughflow in the Indonesian Seas is semigeostrophic, thus bypassing many of the problems inherent in estimating the throughflow. Using the annual mean wind stress climatology of *Hellerman and Rosenstein* [1983] for his analysis, Godfrey obtained an annual mean transport estimate of 16±4 Sv. This estimate for the ITF transport is somewhat larger than the estimates of annual mean transport made from hydrographic measurements, which cluster around 12 Sv. Part of this discrepancy is undoubtedly due to the fact that the zonal component of the *Hellerman and Rosenstein* [1983] wind stress climatology is known to be too strong in the tropics, which would lead to an overestimate of the ITF transport.

2.4. Previous Modeling Studies

Liu et al. [1994], *Lu and McCreary* [1995], *Gu and Philander* [1997], and *Rothstein et al.* [1998] have studied Pacific equatorial thermocline ventilation due to intergyre exchange using ocean models with varying degrees of vertical and horizontal resolution. However, all of these studies neglect the effect of the ITF by using a closed Pacific domain. There are also two global modeling studies that are relevant to our discussion, as they address the influence of the ITF on thermocline circulation within the Pacific Ocean. *Hirst and Godfrey* [1993] used a relatively coarse resolution global version of the Modular Ocean Model (Δx=2.8° longitude, Δy=1.6° latitude, with six layers in the upper 500 m) in order to compare a model run that allowed for ITF with a model run that did not allow for ITF. For their run with an open ITF, a sill depth of 800 m was chosen for the Indonesian Straits, and the passage was given a minimum width of four model grid points. The annual mean ITF transport was determined by the model to be 17.1 Sv with the run for which a sill depth of 800 m was used.

The *Hirst and Godfrey* [1993] model runs were forced with annual mean wind stresses, and the formulation of *Han* [1984] was used to calculate surface heat fluxes. They found that for the case where the ITF was open, the sea surface temperatures (SSTs) in the central and eastern equatorial Pacific were in excess of 0.4°C colder than they were for the case where there is no ITF. This is a consequence of the oceanic heat transport within their model when the ITF is open; the water exported to the Indian Ocean through the Indonesian passages is warmer than the compensating inflow from the extratropical South Pacific, with the result that the thermocline is cooler than for the case with no ITF.

The corresponding surface heat flux in the central and eastern Pacific was also 15 to 20% larger for the ITF open case (note that *Seager et al.* [1995] have shown that the *Han* [1984] heat flux formulation is likely to underestimate fluxes in this region). In addition, the temperature in the warm pool was slightly cooler for the case of an open ITF, so that the overall temperature gradient across the equatorial Pacific is 1°C higher for the case with an open ITF.

A fundamental limitation of the *Hirst and Godfrey* [1993] study, given our interest in the Pacific pycnocline, is one of resolution. With meridional resolution of 1.6°, the model does not capture the critical scales of the equatorial undercurrent, and thus the ventilation pathways for intergyre exchange and equatorial thermocline ventilation are represented too crudely.

Shriver and Hurlburt [1997] used a version of the Naval Research Laboratory (NRL) model to investigate surface and thermocline flow in the low latitude western Pacific basin. The horizontal resolution used for their study is 0.5°, which is sufficient to resolve the critical scales of both the EUC and low-latitude western boundary currents (LLWBCs), and their study illustrates nicely the deviation of the flow fields for the western Pacific thermocline and surface ocean generated using a nonlinear primitive equation model as opposed to linear Sverdrup dynamics.

Given our interest in the thermal budgets associated with intergyre and interbasin exchange, the most significant shortcoming of the *Shriver and Hurlburt* [1993] study is that their model does not include thermodynamics. Their focus was on circulation pathways in the upper Pacific Ocean connecting the ACC to the ITF, and thus they ignored thermal budgets associated with heat transports within the thermocline and buoyancy forcing at the sea surface. Also, the model used for the Shriver and Hurlburt study has only six layers in the vertical, and much of the thermocline flow is confined to the single layer just below the surface layer. We shall see that for models with high resolution, intergyre exchange between the subtropics and equatorial upwelling regions favors the western boundary route for deeper isopycnals and the interior ventilation pathway for shallow isopycnals.

3. Model Description

The model runs discussed herein are designed to test the sensitivity of the mixing ratio of northern and southern component subtropical thermocline water in the equatorial undercurrent to the opening and closing of the ITF. For the case where the ITF is open, the geometry of the throughflow region is highly simplified, and the barotropic transport around Australia is imposed rather than part of the solution. Thus configured, this process study is meant to convey the importance of including the ITF in ocean models that focus on intergyre exchange for the Pacific Ocean.

3.1. Circulation Model

The primitive equation Lamont Ocean-AML (Atmospheric Mixed Layer) Model (LOAM) is used for this study. This is a level version of the *Gent and Cane* [1989] model, which includes a barotropic solver [*Naik et al.*, 1995] with realistic bathymetry. A Lorenz four cycle is used for time differencing, and model calculations are performed on an A grid.

For surface momentum forcing the seasonal wind stress climatology of *daSilva* [1994] is used. The heat flux component of surface buoyancy forcing is calculated using the AML model of *Seager et al.* [1995], which now includes a parameterization for wintertime storm tracks in the extratropics (described by Hazelege et al., manuscript in preparation, 1999). Sea surface salinities are relaxed to the *Levitus et al.* [1994] monthly climatology with a restoring time constant of 1 month.

Two different horizontal domains were used for this study and are shown in Figure 3. The first (Figure 3a) does not allow for any flow around Australia and thus does not permit any ITF transport. The second domain (Figure 3b) does account for an ITF. A channel representing the Indonesian Straits connects the equatorial Pacific and Indian Oceans. The channel has simplified geometry and has a constant depth of 800 m, which is approximately the same depth as that used in the study of *Hirst and Godfrey* [1993].

Although our representation of the throughflow region is simplified, it is justified a postiori, in that the vertical structure of the mean transport, with maximum transport near 100 m depth and most of the transport occurring in the upper 400 m, is in accord with observations. Within the sliver of the Indian Ocean included in the model domain, the temperature [*Levitus and Boyer*, 1994] and salinity [*Levitus et al.*, 1994] fields are relaxed to seasonal values on a timescale of 30 days. This is necessary to maintain the baroclinic structure of the flow in the channel.

As the focus of this study is intergyre exchange, horizontal grid stretching has been used to achieve high resolution in dynamically sensitive regions. The meridional and zonal resolution is shown graphically in Figure 4. The meridional resolution (Figure 4a) is approximately 1/3° along the equator and falls off to ap-

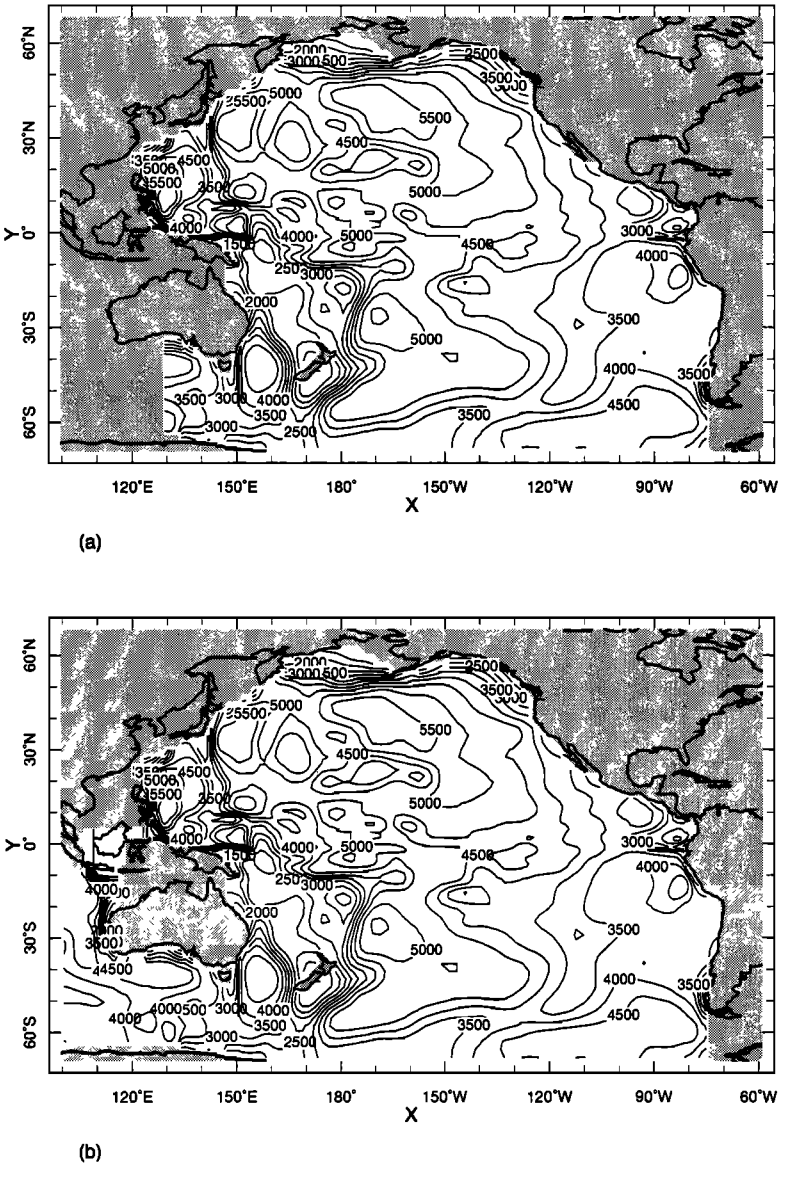

Figure 3. Model domain and bathymetry (a) for case with no Indonesian Throughflow (ITF) and (b) for cases where ITF transport is imposed through barotropic solver.

proximately 2° in the extratropics. The zonal resolution (Figure 4b) is about 1° in the longitude bands of the Mindanao Current, the NGCUC, and the Peru upwelling, with resolution falling off to slightly less than 2° for most of the ocean interior. There are 30 layers in the vertical, 15 of which are in the upper 300 m. High vertical resolution within the thermocline is necessary for the intergyre exchange problem, since water parcels that subduct in the subtropics and upwell along the equator can attain a depth of several hundred meters en route.

Lateral mixing of temperature and salinity is performed using a modified version of the *Griffies et al.* [1998] implementation of the *Redi* [1982] isopycnal mixing tensor, and adiabatic eddy-induced transport of these tracers is accomplished using a modified version of the *Griffies* [1998] implementation of the *Gent and McWilliams* [1990] scheme. As a stretched grid is used for the model runs discussed here, the lateral mixing coefficients have been chosen to vary linearly with horizontal resolution, so that the larger coefficients needed in the extratropics where the resolution is slightly greater than 2° do not compromise the solution in regions where resolution is less than 1°. The coefficient corresponding to both the isopycnal mixing and the eddy-induced transport velocity is approximately 200 $m^2\ s^{-1}$ where resolution is 1/3° and approximately 1600 $m^2\ s^{-1}$ where resolution is larger than 2°. The model sensitivity to this coefficient will be addressed in a further study.

Shapiro filtering is used on the momentum equations, as described by *Gent and Cane* [1989]. In addition, momentum is diffused laterally using a coefficient of 1500

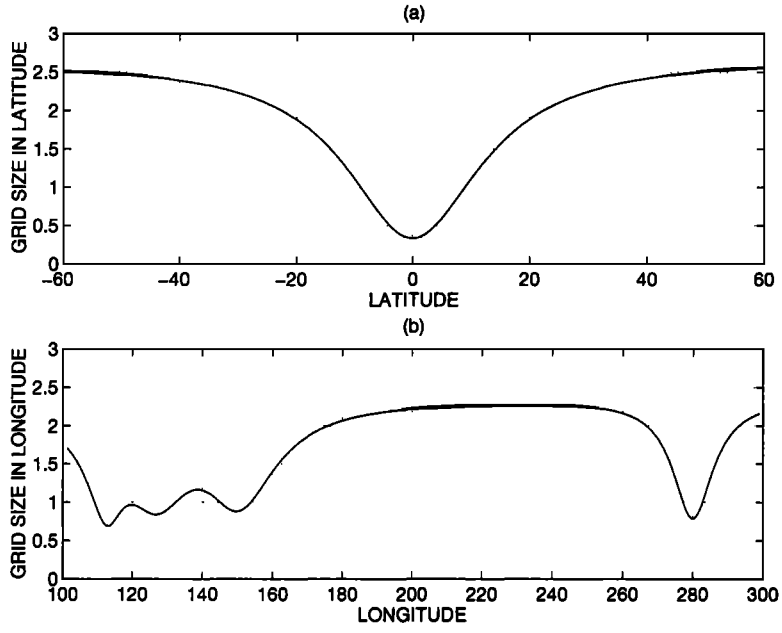

Figure 4. Model (a) meridional and (b) zonal resolution.

$m^2 s^{-1}$. This viscosity decays in the vertical from its full value at the sea surface with an e-folding depth of 200 m. This value was chosen to tune the structure of the model's equatorial undercurrent, as with only Shapiro filtering, the undercurrent is too strong and outcrops at the surface east of the dateline in the annual mean. The physical justification for this parameterization is that high-frequency meridional winds in the equatorial Pacific in the real world lead to a meridional mixing of momentum in the upper ocean across the equator and that this effect will not be captured for ocean models forced with monthly mean wind climatologies. This value of momentum diffusion is rather small, and its effect is only felt in the EUC, where the resolution is high and shears are high. For vertical mixing, in addition to convective adjustment, the mixing parameterization of *Pacanowski and Philander* [1981] is used, with a uniform background diffusivity of 0.1 $cm^2\ s^{-1}$.

Three model runs were made using the the geometry shown in Figure 3 with seasonal forcing: (1) No ITF, with seasonal winds; (2) 10 Sv of imposed ITF, with seasonal winds; and (3) 20 Sv of imposed ITF, with seasonal winds Case (1) uses the domain shown in Figure 3a, and cases (2) and (3) use the geometry shown in Figure 3b. In cases (2) and (3) the time-invariant barotropic ITF transport is imposed through the model's barotropic solver.

For each run discussed here, the model is initialized with temperature and salinity fields from *Levitus and Boyer* [1994] and *Levitus et al.* [1994], respectively. The model is spun out for 10 years in a robust diagnostic mode with a time relaxation constant of 1 year. After this spin-up period, tracer initialization and forcing occur, and the model is integrated for 40 more years.

3.2. Initialization and Forcing of Idealized Tracers

Two idealized tracers are advected on line for the model runs, which impose 0, 10, and 20 Sv of ITF transport, and are used to illustrate mixing ratio of northern to southern component water in the equatorial thermocline. One of the tracers represents a Northern Hemispheric tracer, and the other represents a Southern Hemispheric tracer. Initially, the tracer concentration is set equal to zero everywhere, and the tracer concentration is clamped to a value of 1 poleward of 18° in the respective hemispheres as the model integrates. This formulation is similar to that of *Lu and McCreary* [1995], except that we treat the northern and southern ventilation tracers separately. The advection scheme used for passive tracers is identical to that used for temperature and salinity in the circulation model, and the same mixing parameterizations that operate on temperature and salinity (namely lateral diffusion and the eddy-induced transport) are also used for the passive tracers.

4. Results

4.1. Model Flow Fields

For both the 10 and 20 Sv cases the transport in the channel separating the Pacific and Indian Oceans is maximum at 90 m depth. This is consistent with the observed vertical structure of flow in the Indonesian Straits, where flow is observed to be maximum at approximately 100 m depth (A.L. Gordon, personal communication, 1998). This is significant, because the model is siphoning off water at the correct density horizon for the Pacific Ocean, despite its simplified representation of the geometry of the Indonesian Straits.

The flow at a depth of 90 m is shown in Figure 5a for the case with no ITF and in Figure 5b for the case with 10 Sv of imposed ITF transport. The 10 Sv of ITF siphons off a significant fraction of the southward flowing Mindanao Current water toward the Indian Ocean. An important difference between the two cases lies in the flow along the northern coast of New Guinea. The strong retroflection just north of New Guinea for the case with the open throughflow is consistent with the flow fields measured during the WEPOCS II survey at 143°E [*Tsuchiya et al.*, 1989]. At 195 m depth in the thermocline, for the case with no ITF (Figure 5c), nearly all of the equatorward flowing Mindanao Current feeds the EUC, while with 10 Sv of ITF (Figure 5d) the Mindanao Current splits at approximately 4°N and its contribution to the EUC is significantly diminished.

Next we consider the zonal flow across two transects in the thermocline of the western Pacific. The first of these is along 142°E between 3°S and 7°N, which corresponds to the WEPOCS II section described by *Tsuchiya et al.* [1989]. The flow across this section for the case with no ITF (Figure 6a) shows maximum zonal flow within the EUC of 55 cm s^{-1}, centered just north of the equator. The flow across this section for the case with 10 Sv of ITF (Figure 6b) reveals the vertical structure of the retroflection of NGCUC water shown in Figure 5. The strong westward flow within the thermocline along the northern coast of New Guinea is nearly as large as that of the eastward flowing EUC and is consistent with the findings of the WEPOCS program.

The meridional component of flow across 5.7°S is shown in Figure 6c for the case with no ITF and in Figure 6d for the case with 10 Sv of ITF. As the ITF transport increases, so does the influx of water from the South Pacific across 7°S, as required by continuity. Significantly, the compensation occurs primarily within the NGCUC.

4.2. Model Results for Hemispheric Tracers

The Northern and Southern Hemispheric tracer distributions for the case with no ITF are shown projected onto the σ_θ=25.0 isopycnal surface in Figures 7a and 7b. These plots represent snapshots 10 years after tracer initialization. The Northern Hemisphere tracer can be seen to access the equator primarily through advection within the Mindanao Current. Along the equator the

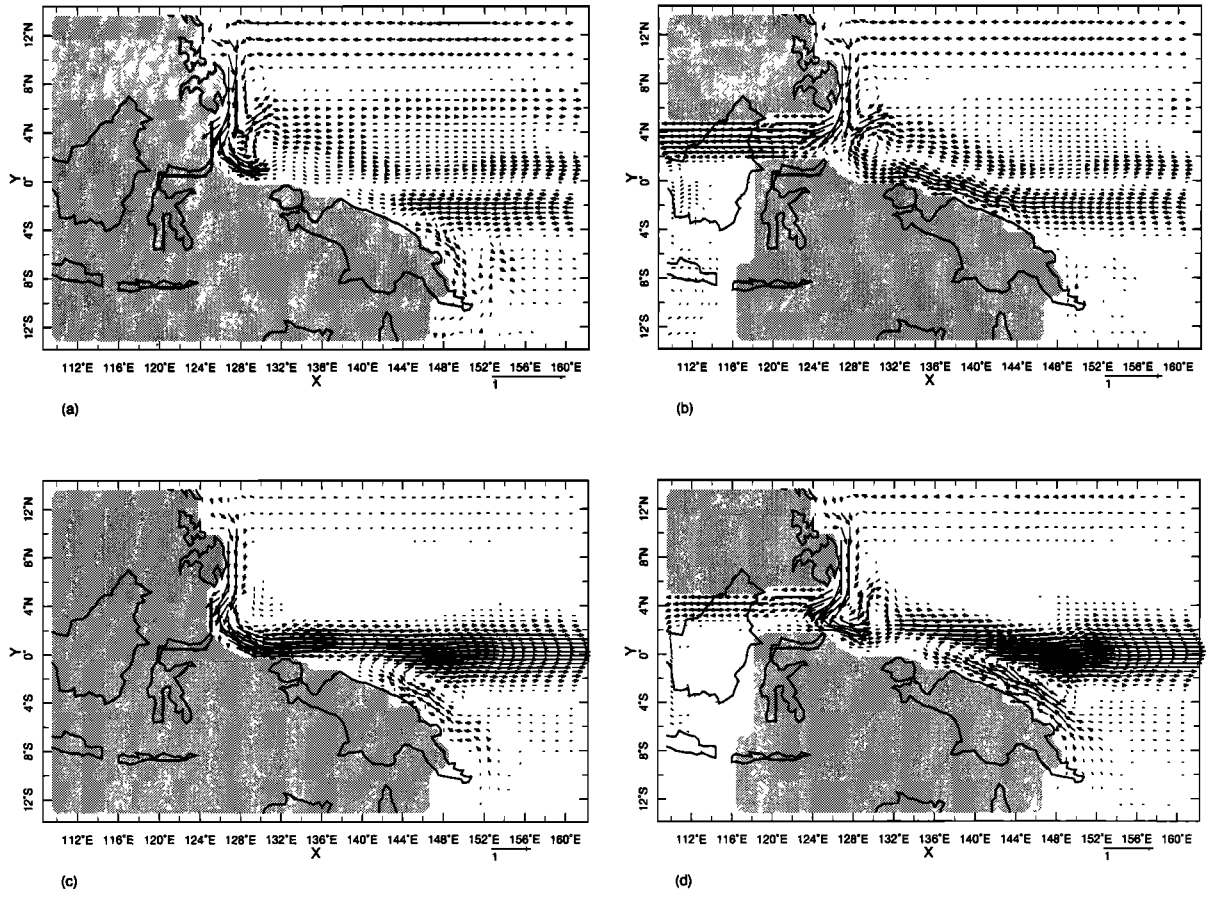

Figure 5. Vector plots of flow fields at 90 and 195 m depth in the western Pacific, showing flow at (a) 90 m depth for case with no ITF, (b) 90 m depth for case with 10 Sv of imposed ITF, (c) 195 m depth for case with no ITF, and (d) 195 m depth for case with 10 Sv of imposed ITF.

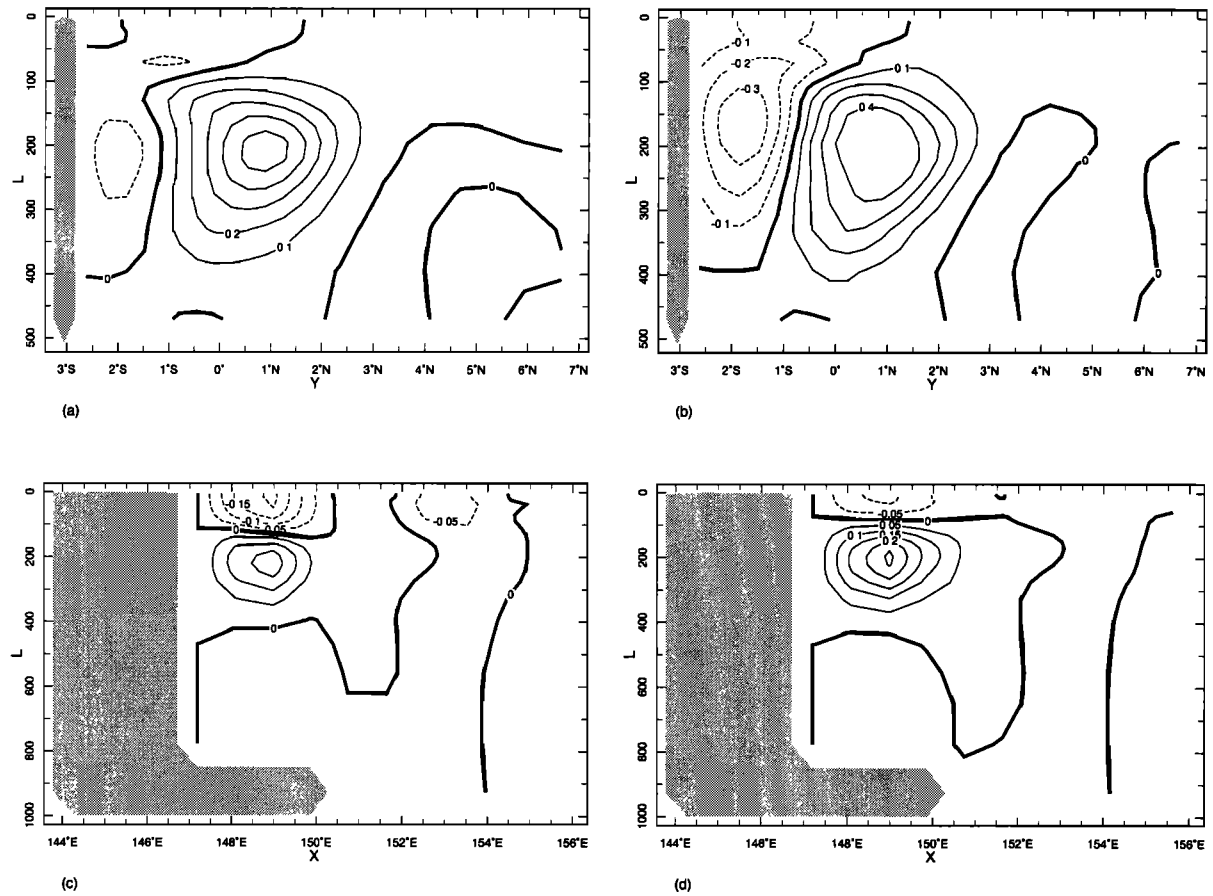

Figure 6. Annual mean zonal velocity as a function of latitude and depth at 142°E for the case (a) with no ITF and (b) with 10 Sv of ITF. The contouring interval for Figures 6a and 6b is 0.1 m s^{-1}. Annual mean meridional velocity across 5.7°S for the case (c) with no ITF and (d) with 10 Sv of ITF. The contouring interval for Figures 6c and 6d is 0.05 m s^{-1}.

concentration of the Northern Hemisphere tracer is significantly larger than that of the Southern Hemisphere tracer.

The unventilated region along 10°N in the eastern Pacific in Figure 7a is the shadow zone of the North Pacific subtropical gyre and is an oxygen-minimum zone in the real ocean. The minimum zone along 4°N seen stretching from the eastern edge of the Mindanao Current across the basin has been attributed by *Lu and McCreary* [1995] to the potential vorticity barrier posed by the Inter Tropical Convergence Zone (ITCZ).

For the Southern Hemisphere tracer shown in Figure 7b, both the interior and western boundary ventilation routes contribute to the equatorial undercurrent. The interior ventilation route penetrates closest to the equator at 140°W.

The tracer distributions for the case with 10 Sv of imposed ITF after 10 years are shown in Figures 7c and 7d. With the throughflow region open, Northern Hemisphere tracer concentrations are lower along the equator than they were for the case with no throughflow. Much of the tracer that flows south within the Mindanao Current has now been diverted into the throughflow and can be seen exiting the Pacific in the throughflow region.

The Southern Hemisphere tracer in the 10 Sv case (Figure 7d) shows concentrations in the equatorial undercurrent that are significantly larger than they were for the case with no ITF. The maximum in tracer concentration along the equator can be traced back to the NGCUC at the western boundary, which is the dominant equatorial ventilation pathway from the Southern Hemisphere on this isopycnal horizon. The case with 20 Sv of imposed ITF is shown in Figure 7e and 7f. The overall pattern for both hemispheres remains the same, although the tracer concentration along the equator is once again diminished for the northern tracer and enhanced for the southern tracer.

In Figure 8 we consider meridional sections of tracer concentration at 150°W for the three model runs. For the case with no ITF the Northern Hemisphere tracer (Figure 8a) is dominant at all depths within 2° of the equator. The maximum concentration of Northern Hemisphere tracer within the undercurrent is three times larger than the maximum concentration of South-

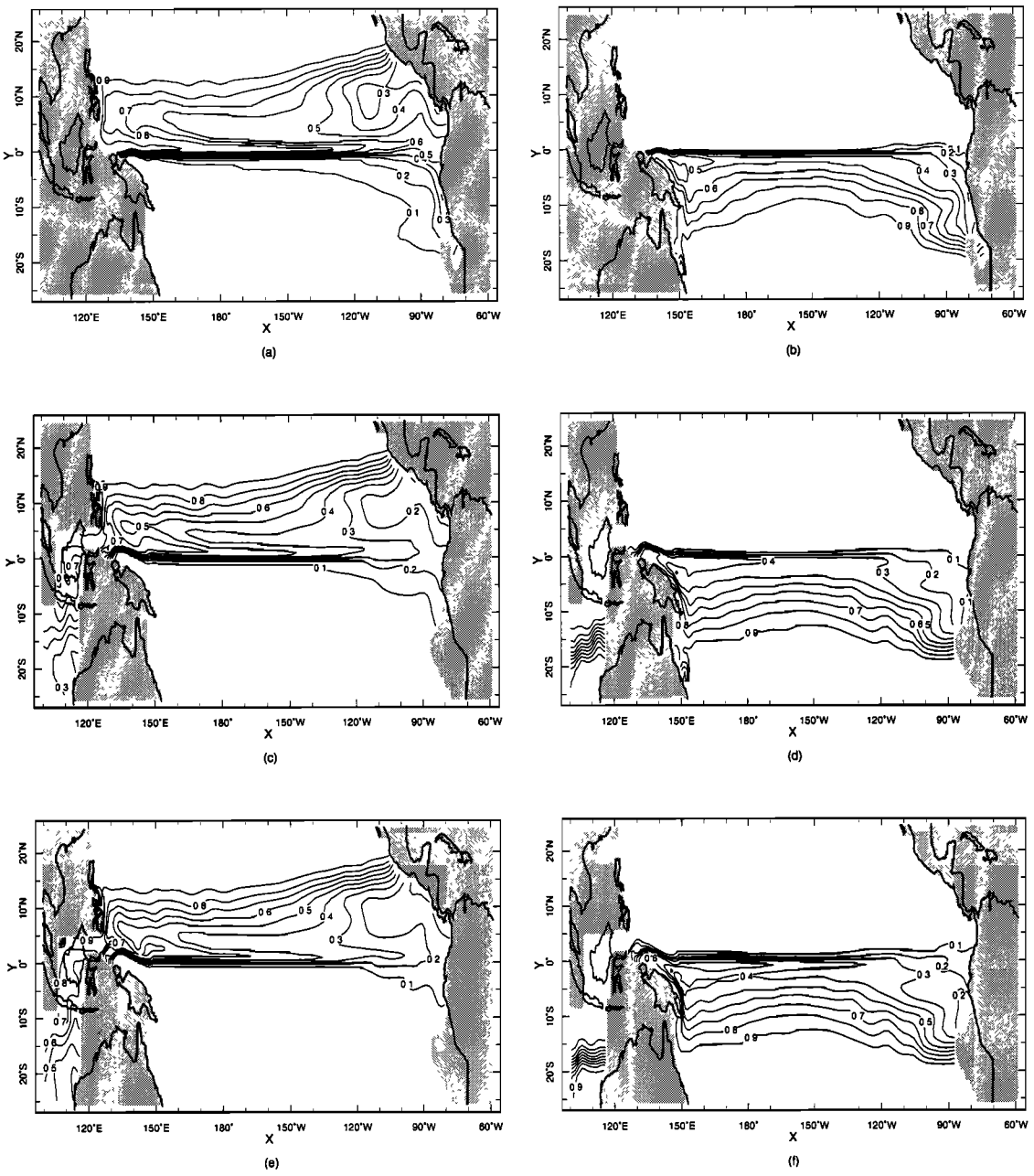

Figure 7. Tracer distribution on the σ_θ=25.0 surface after 10 years, showing (a) the Northern Hemisphere tracer for the case with no ITF, (b) the Southern Hemisphere tracer for the case with no ITF, (c) the Northern Hemisphere tracer for the case with 10 Sv ITF, (d) the Southern Hemisphere tracer for the case with 10 Sv ITF, (e) the Northern Hemisphere tracer for the case with 20 Sv ITF, and (f) the Southern Hemisphere tracer for the case with 20 Sv ITF.

ern Hemisphere tracer. The Northern Hemisphere tracer concentration within the EUC is a pronounced local maximum (with tracer concentration in excess of 0.9) associated with the eastward transport of the EUC, whereas for the Southern Hemisphere there is no local maximum of tracer concentration within the EUC (Figure 8b). The Southern Hemisphere tracer is largely confined to the region south of 2°S.

For the run that imposed 10 Sv of ITF (Figures 8c and 8d), the maximum in the concentration of the Northern Hemispheric tracer along the equator is less than 0.7, and there is a significant reduction in the off-equatorial concentration as well when compared to the case with no ITF. The Southern Hemispheric tracer shows elevated concentrations between 2°S and 2°N relative to the case with no ITF, and the Southern Hemispheric tracer now accesses the EUC. With 20 Sv of imposed ITF the maximum concentration of Northern Hemispheric water in the EUC is now less than 0.6, and there is now an isolated local maximum of Southern

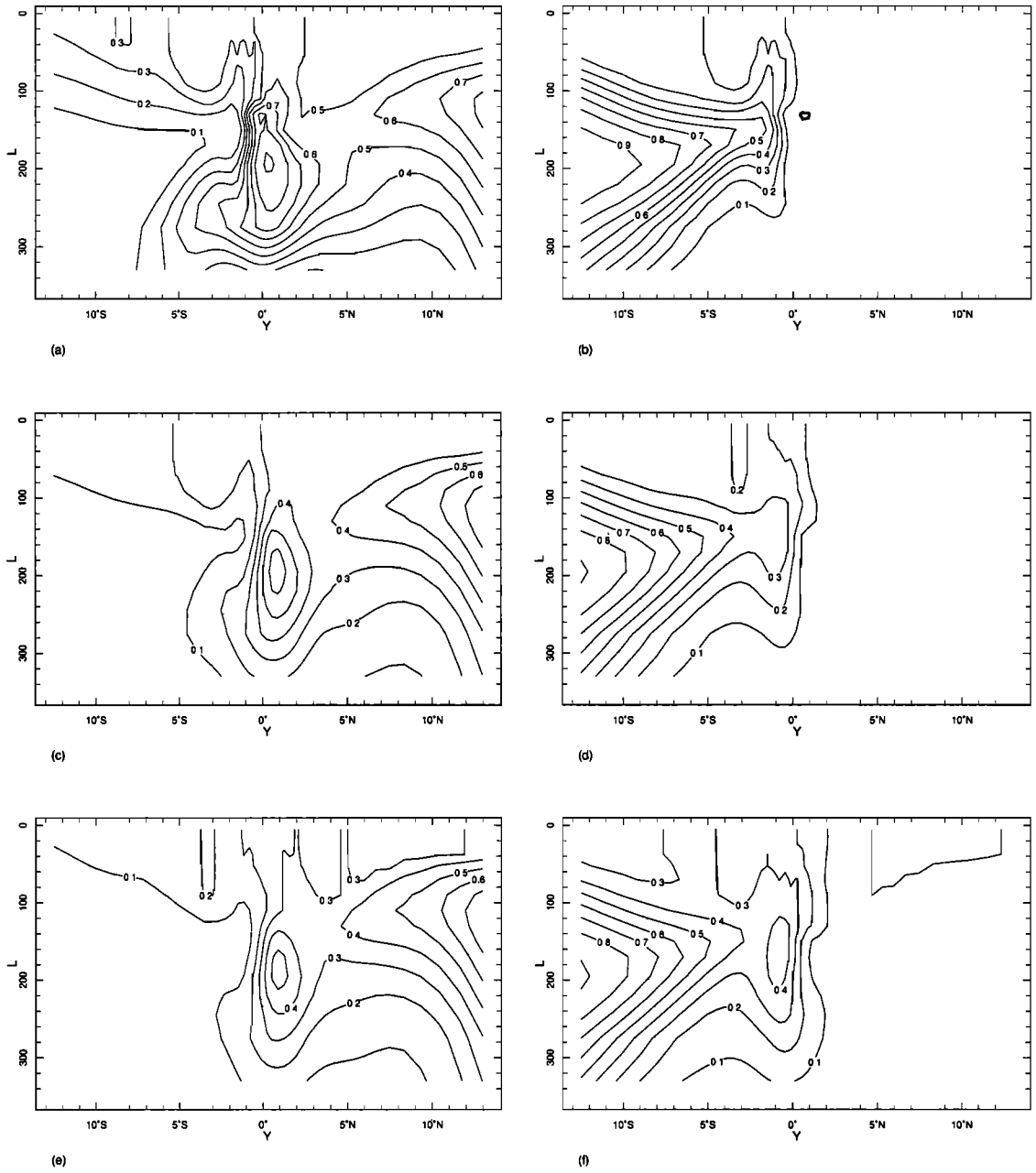

Figure 8. Tracer distribution at 150°W after 20 years of model integration, showing (a) the Northern Hemisphere tracer for the case with no ITF, (b) the Southern Hemisphere tracer for the case with no ITF, (c) the Northern Hemisphere tracer for the case with 10 Sv ITF, (d) the Southern Hemisphere tracer for the case with 10 Sv ITF, (e) the Northern Hemisphere tracer for the case with 20 Sv ITF, and (f) the Southern Hemisphere tracer for the case with 20 Sv ITF.

Hemispheric water within the EUC. In addition, there is some cross-equatorial transport of Southern Hemisphere tracer into the NECC, which is consistent with observations [*Gordon*, 1995].

The evolution with time of the mixing ratio of southern component to northern component waters in the equatorial thermocline for the case with no ITF, the case with 10 Sv of ITF, and the case with 20 Sv of ITF, is shown in Figure 9. For all three cases the mixing ratio is smallest after 5 years, as the initial signal from the Northern Hemisphere ventilates more rapidly than the signal from the Southern Hemisphere. The mixing ratio changes very little after year 20 for all three cases.

The results for the hemispheric tracer are summarized in Table 1. A rectangular box ranging in depth from 50 to 150 m and in latitude from 2°N to 2°S has been chosen to correspond to the equatorial thermocline. Within this box the average concentration of both the northern and southern tracer has been tabulated for the end of the 20th year of model integration.

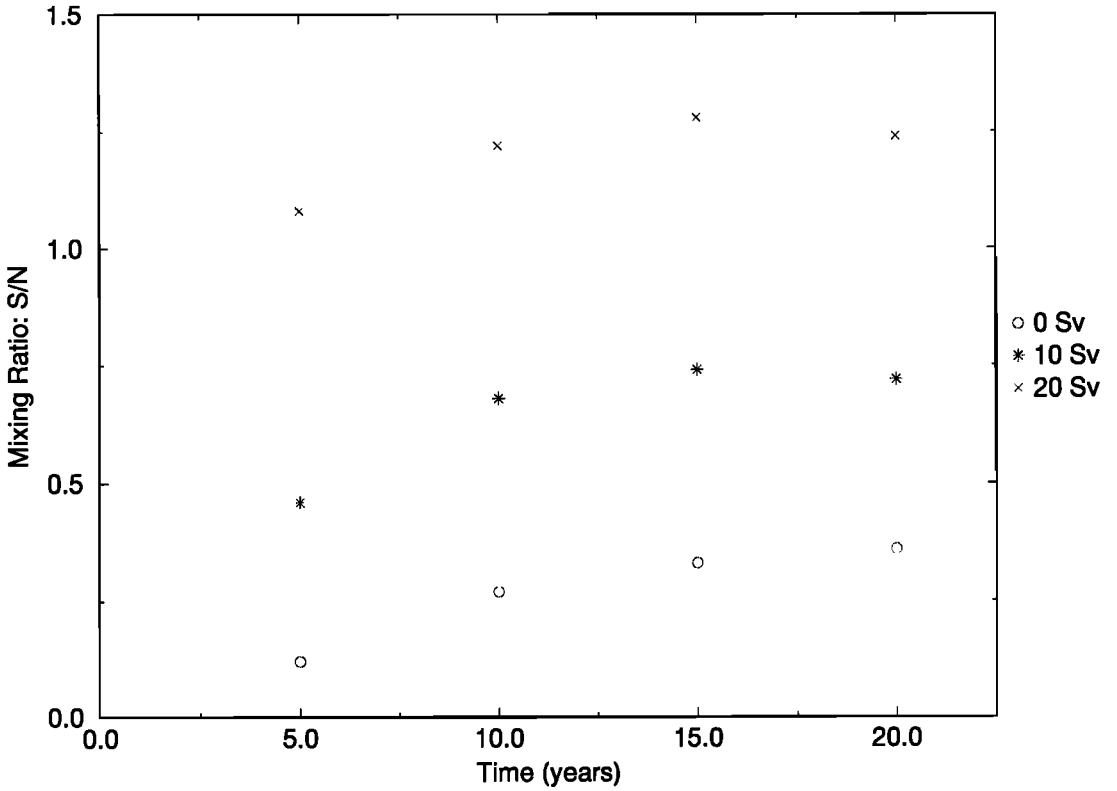

Figure 9. Evolution of mixing ratio of southern to northern component water in Equatorial Undercurrent for three model runs over 20 years (Lamont Ocean Model, level version of *Gent and Cane* [1989]). Although the system has not yet reached steady state, this timescale is longer than the 10-15 year ventilation 'age' of equatorial pycnocline water inferred from chlorofluorocarbon measurements in the Pacific [*Warner et al.*, 1996].

In Figure 10 the mixing ratio of the Northern Hemispheric tracer to the Southern Hemisphere tracer is shown as a function of depth and longitude after 20 years for each of the three cases (0, 10, and 20 Sv). For each case the mixing ratio has been averaged between 2°N and 2°S. With 0 Sv of ITF (Figure 10a), we see that the mixing ratio is consistently greater than 2 over the equatorial pycnocline. However, this plot also reveals significant zonal and vertical structure, with the ratio tending to increase below 100 m depth. The largest gradients near 140°E, between 100 and 300 m depth, are associated with the retroflection shown in Figure 5.

The case for 10 Sv of ITF (Figure 10b) also reveals significant vertical and zonal structure. Here the mixing ratio in the upper 200 m is between 1 and 2 for most of the region between 150°E and the eastern boundary, with the relative contribution of the Northern Hemispheric tracer increasing to the east and with depth. With 20 Sv of ITF (Figure 10c) the ratio is less than 1 over most of the region. As with the case with 10 Sv, the relative contribution of the northern component water increases to the east and with depth.

The barotropic stream function calculated by the model is nearly identical over the interior regions of the Pacific for the three cases (0, 10, and 20 Sv of imposed ITF) discussed here. The Sverdrup circulation across 30°S is roughly 30 Sv for each case. However, the cases differ in their calculated transport of the East Australia Current, the western boundary current of the South Pacific subtropical gyre. For the 0 Sv of imposed ITF transport, the recirculation within the East Australia Current is roughly 30 Sv, whereas with 10 or 20 Sv of imposed ITF transport, the east Australia Current is diminished by an amount equal to the imposed ITF transport. This is a consequence of continuity and

Table 1. Percentage of Different Component Waters After 20 Years as a Function of Imposed Indonesian Throughflow Transport

Component	0 Sv	10 Sv	20 Sv
Northern Hemisphere	66	43	33
Southern Hemisphere	24	31	41
Other	10	26	26

The percentages are calculated by taking the average concentration of the hemispheric tracers within a box bounded in the vertical by the 50 and 150 m depth horizons and by 2°N and 2°S meridionally over the entire equatorial Pacific. "Other" is calculated by subracting the sum of the two hemispheric tracer concentrations from unity for each run.

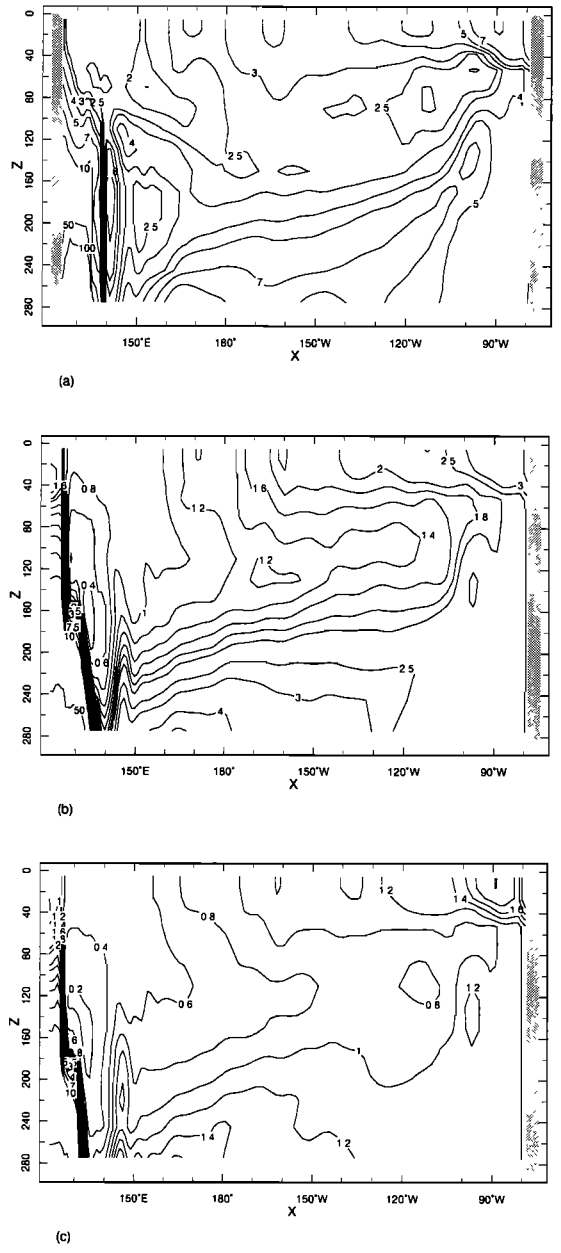

Figure 10. The mixing ratio of northern to southern component water plotted as a function of longitude and depth along the equator. The plotted quantity represents an average over the latitude range 2°N to 2°S. Shown are cases with (a) 0 Sv ITF, (b) 10 Sv ITF, and (c) 20 Sv ITF. The contouring levels for the mixing ratio are 0.1, 0.2, 0.4. 0.6, 0.8, 1.0, 1.2, 1.4, 1.6, 1.8, 2, 2.5, 3, 4, 5, 7, 10, 50, 100.

the fact that the interior circulation is determined by Sverdrup dynamics.

5. Variability in Hydrographic Data

The mechanism proposed by *Deser et al.* [1996], *Gu and Philander [1997]*, and *Zhang et al.* [1998] for changing the thermal structure of the equatorial pycnocline focuses on temperature anomalies of order 0.5°C advecting into the equatorial region from poleward of 30°. In essence, this involves a temperature anomaly advected by a mean flow, eventually impacting the temperature of the thermocline downstream. It is known, however, that the equatorial circulation is quite variable. Thus it is worth considering the basin-scale time mean temperature gradients within the pycnocline ($\nabla\overline{T}$ of (1)) corresponding to the salinity distribution shown in Figure 2.

The temperature distribution on the σ_θ=25.0 isopycnal surface between 30°N and 30°S calculated from the *Levitus et al.* [1994] and *Levitus and Boyer* [1994] annual mean temperature and salinity fields is shown in Figure 11a. As before, the σ_θ=25.0 surface is chosen because it corresponds to the approximate density horizon of the core of the equatorial undercurrent. A 2°C meridional temperature gradient exists across the equator. Minimum temperatures of less than 15°C are found within the California Current off Baja California near 120°W. Maximum temperatures in excess of 22°C can be found between 10° and 20°S across the South Pacific subtropical gyre. As with the hemispheric salinity gradients in Figure 2, the meridional temperature gradients on this isopycnal surface are due to differences in surface freshwater fluxes in the Northern and Southern Hemispheres.

Figure 11b shows a zonally averaged plot of temperature as a function of latitude and density from the *Levitus and Boyer* [1994] climatology for the Pacific. The 2°C change in zonally averaged temperature between 8°N and 8°S on the σ_θ=25.0 surface can be seen to exist over the density range σ_θ=24.0 to 26.5. As the horizontal smoothing radius for the *Levitus and Boyer* [1994] and *Levitus et al.* [1994] data sets is of order 500 km, we cannot expect to resolve fronts or features on finer scales than this. This temperature distribution represents the $\overline{T}$ of (1), and for the real ocean, $\partial\overline{T}/\partial y$ within the equatorial thermocline is of order 2°C/1600 km along isopycnal surfaces.

Having considered the large-scale time mean temperature distribution on an isopycnal surface within the Pacific pycnocline, we turn our attention to a transect at 165°E that was sampled at least twice per year between 1984 and 1990. The data set discussed here consists of conductivity-temperature-depth (CTD) casts from 10 cruises by the Surveillance Trans-Océanique du Pacifique (SURTROPAC) program conducted by the Institut Français de Recherche Scientifique pour le Développement en Coopération (ORSTOM) group from New Caledonia, three cruises from the Production Pélagique dans le Pacifique (PROPPAC) program, and seven cruises from the United States/People's Republic of China (US/PRC) program. The time averaged fields along this transect have been described by *Gouriou and Toole* [1993].

Figure 12 shows a scatterplot of temperature and salinity measurements (indicated by open circles) for

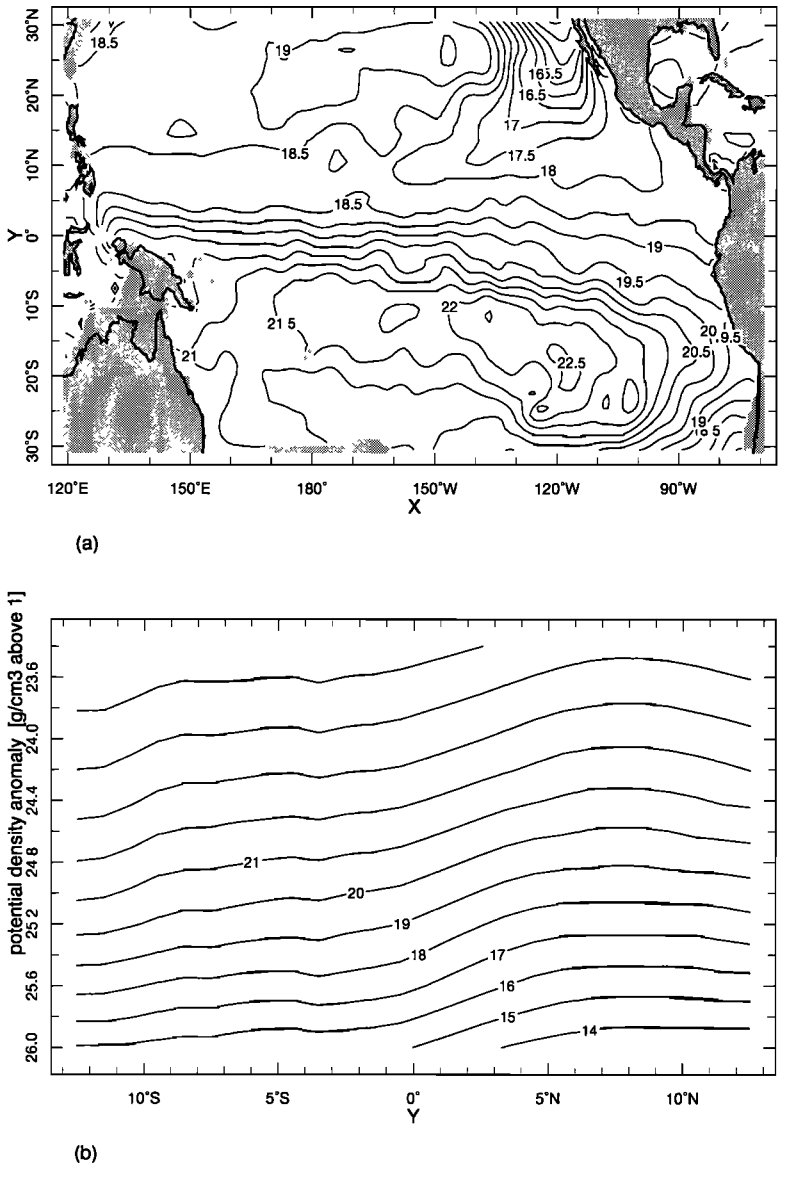

Figure 11. Temperatures from the *Levitus and Boyer* [1994] annual mean climatology (a) of the σ_θ=25.0 isopycnal surface and (b) as a function of latitude and density (zonally averaged).

the CTD measurements for equatorial stations (165°E, 0°N) for all of the cruises combined. The corresponding σ_θ surfaces are superposed on the figure, and the Mindanao Current (cold and fresh) and New Guinea Coastal Undercurrent (warm and salty) end-members are shown as stars. Figure 12 shows that the temperature variability exists on the equator when viewed isopycnally, although this plot tells us nothing about the phase of the variability. For the density range between σ_θ=25.0 and 26.0, which roughly corresponds to the equatorial undercurrent, the variance is of order 1°C. Also worth noting is the fact that the mean mixing ratio of southern to northern component water is slightly larger than 0.5 between σ_θ=25.0 and 26.0 and increases with depth, so that by σ_θ=27.0 the source of the water at this location is dominated by the southern component.

Figure 13 shows a Hovmoeller diagrams for temperature as a function of latitude and time for this data set along the isopycnal surface σ_θ=24.5. Along this surface, which lies in the upper part of the undercurrent, the temperature gradient of approximately 2°C can be seen across the equator. Between 2°S and 2°N, which corresponds to the latitude range of the Equatorial Undercurrent, there is low-frequency variability, with cooler temperatures measured in late 1987 followed by warmer temperatures. There is also low-frequency temperature variability within the South Equatorial Current at approximately 4°S, where the temperature in early 1987 is approximately 1°C cooler than in early 1988.

6. Discussion

We have seen from our modeling results that the equatorial thermocline circulation is indeed quite sen-

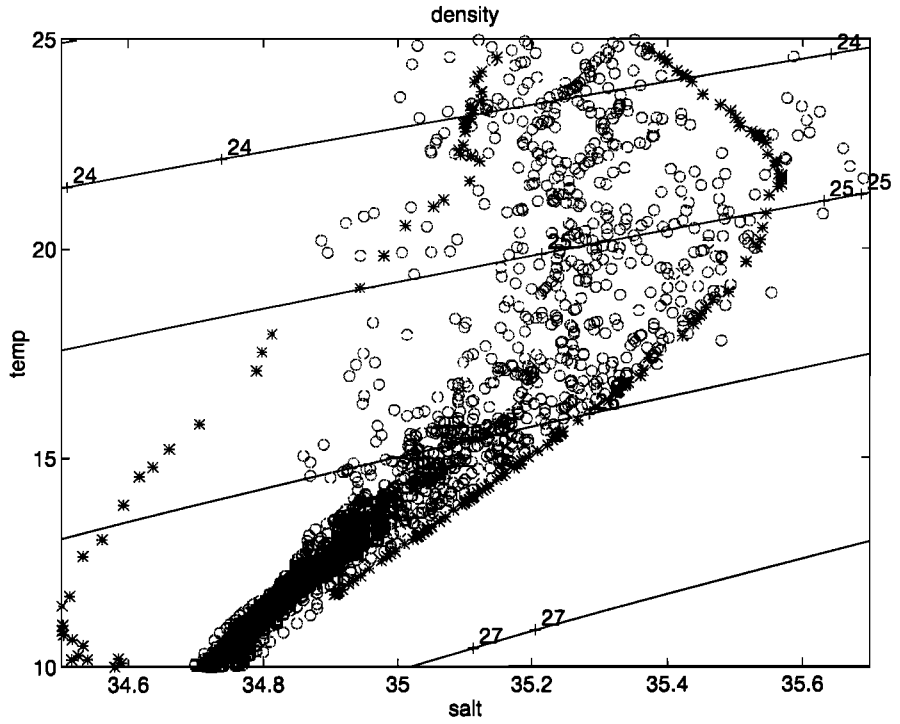

Figure 12. T/S scatterplot for conductivity-temperature-depth (CTD) data collected at 165°E, 0°N (open circles) between 1984 and 1990 (Data courtesy of John Toole, Woods Hole Oceanographic Institution, 1998). The stars represent CTD measurements from the low-latitude western boundary current (LLWBC) regions, namely, the fresh Mindanao Current (left) for the northern hemisphere, and the coast of New Guinea for the southern hemisphere (right). Contours of potential density anomaly are also included.

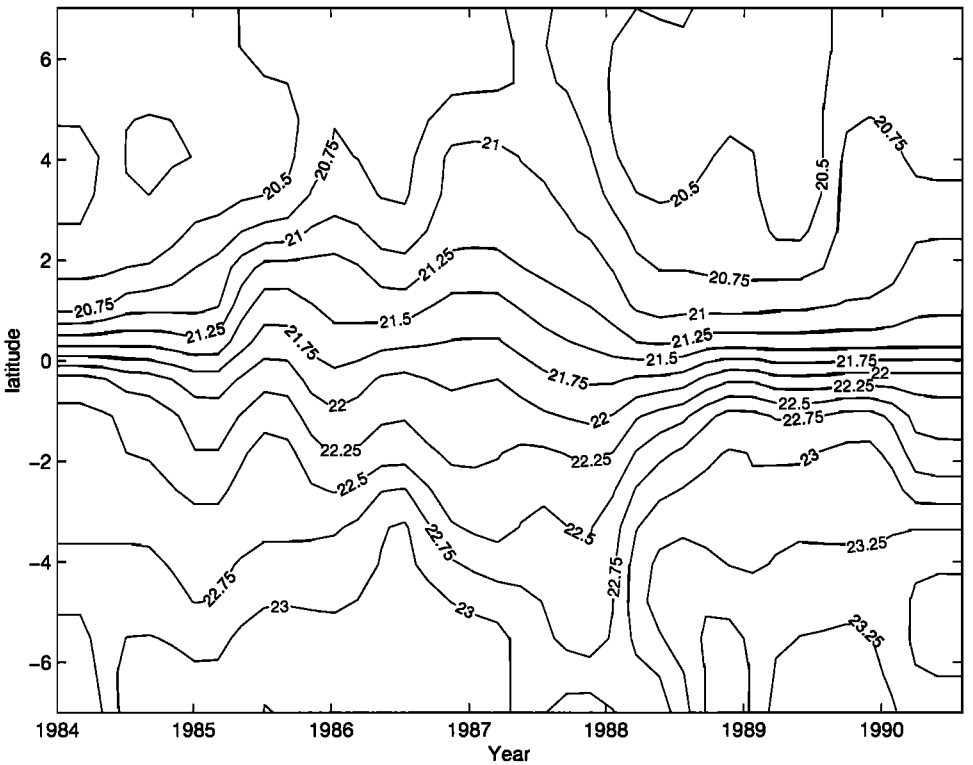

Figure 13. Temperature (time, latitude) at 165°E on σ_θ=24.5 between 1984 and 1990. These CTD data are courtesy of John Toole, Woods Hole Oceanographic Institution, and have been interpolated to isopycnal surfaces.

sitive to the transport of thermocline water from the Pacific to the Indian Ocean through the Indonesian Straits. Only when the imposed transport is between 10 and 20 Sv does the mixing ratio of the Southern to the Northern Hemispheric tracer become larger than 1 for the equatorial pycnocline, in agreement with what is seen in the T/S scatterplot of Figure 12. Assuming that the mixing ratio increases approximately linearly with the imposed ITF transport and given the salinity-derived estimate of 1/2 to 2/3 of the thermocline derive from the Southern Hemisphere [*Tsuchiya et al.*, 1989], our results are consistent with Godfrey's estimate of 16 Sv calculated using the Island Rule. However, this value of 16 Sv is approximately 50 per cent larger than the mean values inferred from observations [*Godfrey*, 1996].

For the hemispheric tracers the results for the three runs considered here are consistent with the results of *Lu and McCreary* [1995], insofar as the ITCZ presents a potential vorticity barrier that inhibits interior ventilation from the Northern Hemisphere. The barrier formed by the ITCZ is not impermeable, as interior ventilation does occur for the Northern Hemisphere along isopycnals above the core of the undercurrent. Nevertheless, the ITCZ barrier is responsible for a hemispheric asymmetry, in that interior ventilation occurs more readily from the Southern Hemisphere.

The choice of 18° latitude as the cutoff for the tracer-forcing function was motivated by our interest to be consistent with the model experiment of *Lu and McCreary* [1995]. However, their choice of 18° latitude for their tracer forcing function was motivated by the fact that this is the cutoff latitude for their subduction parameterization. Since this choice of a cutoff latitude does not have special significance for the physical problem of intergyre exchange, the sensitivity of the results presented here to the cutoff latitude of the tracer forcing function will be pursued in our further study.

Continuity requires the ITF transport to be balanced by a cross-equatorial flow of water from the Southern Hemisphere. Southern component thermocline waters do not cross the equator easily in the western or central Pacific; note the strong retroflection along the north coast of New Guinea in Figures 5b and 5d, as well as the fact that the strong equatorial fronts in temperature and salinity are maintained in steady state for the real ocean. Upon reaching the northern coast of Papua New Guinea near 140°E, nearly all of the northwestward flowing NGCUC water retroflects to feed the EUC. Only after traversing the Pacific from west to east within the EUC, upwelling in the eastern Pacific, and undergoing a water mass transformation at the sea surface, is the majority of this southern component water able to enter the Northern Hemisphere.

In a series of ocean model experiments using a closed rectangular domain with idealized winds, *Liu and Philander* [1995] distinguished between "recirculation windows" and "exchange windows" for the subducting regions of the subtropical gyres. For the North Pacific the existence of the ITF adds an additional pathway not available for a closed domain. *Fine* [1985] has pointed out that the tritium measured in the thermocline of the equatorial Indian Ocean during the Geochemical Ocean Sections Survey (GEOSECS) of the 1970s originated in the North Pacific and thus subducted in the "ITF window" of the North Pacific subtropical gyre.

The three model runs considered in this study did not allow for any time variability in the ITF transport. Given that there exists a 2° temperature gradient along isopycnals between the northern and southern component water in the western equatorial Pacific thermocline, as well as strong sensitivity of the mixing ratio of northern to southern component water in the EUC to the transport of the ITF, a question naturally arises: to what extent could real-world variability in ITF transport lead to variability in the thermal structure of the equatorial pycnocline? More specifically, we are interested in investigating the relative magnitudes of the terms in (1) and working quantitatively through the implications for climate variability. This will be investigated in a future study.

As mentioned earlier, *Hirst and Godfrey* [1993] found that eastern equatorial Pacific SSTs are cooler when the Indonesian Throughflow is open in their model. This is despite the fact that for this case, more water is being drawn from the Southern Hemisphere, where we expect temperatures to be warmer for the same isopycnal surface. Hirst and Godfrey attributed this to the water that exits the Pacific thermocline through the ITF coming from a shallower level then the compensating inflow from the South Pacific, with the net effect that the Pacific thermocline shallows for an open ITF.

In this study the SST is also quite sensitive to whether the ITF is open or closed. Figure 14 shows that in the case with 10 Sv of imposed ITF, the annual mean SST is as much as 1°C colder than in the case with no ITF. The difference in SST patterns between the case with 10 Sv of imposed transport and the case with 20 Sv of imposed transport is quite small in comparison. Our results in the eastern equatorial Pacific are consistent with the results of *Hirst and Godfrey* [1993], except that the SST differences are less confined to the equator for our model. This can be attributed in large part to the differences in the surface heat flux parameterization used in the two studies. *Hirst and Godfrey* [1994] used the parameterization of Han [1984], which includes a strong damping term on SST. By using the AML of *Seager et al.* [1995], we have allowed changes in the temperature of the Peru upwelling to propagate into the ocean interior through the influence of the trade winds.

The sensitivity of SST in the tropics to the imposed ITF transport should be understood as the surface expression of a response in the depth of the pycnocline to the ITF. When the ITF is open, the entire equatorial pycnocline is shallower than for the case where the ITF is closed. The changes in SST associated with the changes in pycnocline depth are large enough to more

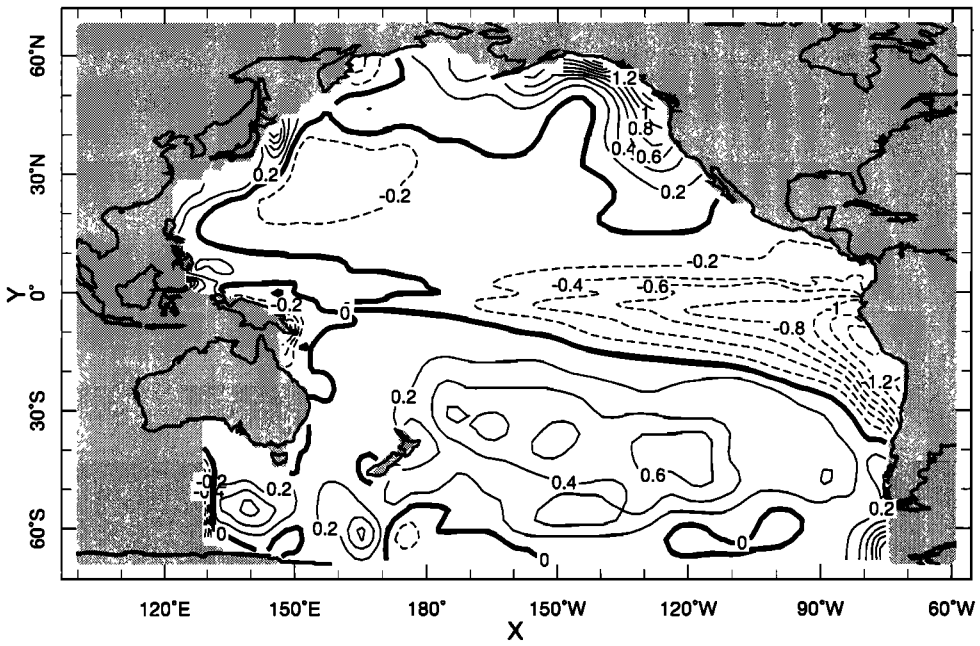

Figure 14. Difference in annual mean SST between case with 10 Sv of imposed ITF and case with no ITF. Units are °C, and negative contours in the Eastern Equatorial Pacific indicate that temperatures are cooler when the ITF is open.

than compensate for the meridional temperature gradients seen on isopycnal surfaces within the pycnocline of Figure 11a. The SST sensitivity poleward of 20° in either hemisphere is not insignificant and again reflects changes in the depth of the pycnocline on a basin-wide scale. The dynamical mechanisms responsible for this strong non local response to changes in ITF transport will be the subject of future investigation.

Another subject for further investigation will be the variation in pycnocline depth with variations in Indonesian Throughflow transport on seasonal to interannual timescales. All the studies discussed ignore seasonal and interannual variability in ITF transport. If the cooler SSTs found in our study (as well as in the *Hirst and Godfrey* [1994] study) for the case where the ITF is open were to correspond to the response of the real ocean to increased throughflow transport, then this would offer a feedback mechanism with potential implications for the ocean thermostat mechanism proposed by *Clement et al.* [1996]. Assuming that the zonal SST gradient increases in response to increased greenhouse forcing, the trade winds respond by increasing in strength, thus increasing the difference in sea level height between the Pacific and Indian Oceans. Owing to the increased pressure head difference between the Pacific and Indian Oceans, the transport of the ITF would increase, thereby cooling the sea surface in the eastern equatorial Pacific, thus constituting a positive feedback.

According to Table 1, approximately 25% of the water within the equatorial pycnocline after 20 years falls into the 'other' category for the two runs that include ITF transport. This raises the question of the extent of diapycnal mixing within the model due to the mixing parameterization of *Pacanowski and Philander* [1981], in our model. For the hemispheric tracers used here, one cannot readily distinguish between cool and fresh water that has been locally entrained from below and subtropical water that is merely slow in accessing the equatorial pycnocline along isopycnal surfaces.

The study of *Lu et al.* [1998], which used a 3-1/2 layer model with an account of the Indonesian Throughflow, suggests that the mixing ratio of southern to northern component water in the equatorial pycnocline should be dependent on the extent of diapycnal fluxes within the equatorial pycnocline. Increased entrainment of water from below the directly ventilated thermocline tends to increase the relative contribution of southern component water. If this is true, then the fact that the ITF required by our model is roughly 50% larger than observations could be a manifestation of diapycnal mixing with the equatorial pycnocline being too small for our model runs. In a future study the hemispheric tracers used here will be generalized such that they tag particular isopycnal layers from each hemisphere. In this way we can quantitatively address the extent of entrainment associated with intergyre exchange.

Two caveats are in order with regard to the comparison of the model and the data. First, our comparison is complicated by the fact that for the model, there is significant zonal structure to the mixing ratio of northern to southern component water in the equatorial thermocline (Figure 10). This zonal structure will also exist when the mixing ratio is evaluated along isopycnal surfaces in the equatorial pycnocline. For the case with 10

Sv of imposed ITF (Figure 10b), there are roughly equal proportions of northern to southern component water in the region to the west of the dateline, which corresonds to the region of sampling used for the salinity-based estimates [*Tsuchiya et al.*, 1989, *Gouriou and Toole*, 1993].

This underscores the need for a more complete analysis of the existing database of hydrographic measurements in the equatorial Pacific thermocline, in order to further our understanding of the sources of upwelling equatorial thermocline water. This should include hydrographic measurements from a range of longitudes across the Pacific in order to better establish the spatial stucture of the mixing ratio in the real ocean as revealed in the salinity field. In our future work we will also incorporate measurements of the transient tracers bomb radiocarbon and bomb tritium in the equatorial thermocline to adress this question (as suggested by *Broecker et al.* [1995]).

The second caveat is that caution must be exercized when using information derived from passive tracers to infer the behavior of temperature and salinity anomalies in the ocean. Some important differences between passive and active tracers have been discussed by *Liu and Huang* [1988]. Nevertheless, our hemispheric tracers provide a useful diagnostic for the sources of the model's equatorial thermocline water for the mean state with climatological forcing, and the results provide motivation for a more careful reassessment of the existing database of hydrographic and transient tracer data.

7. Conclusions

The transport of the ITF strongly influences the ratio of northern to southern component water in the equatorial pycnocline. High-resolution ocean models of Pacific circulation that do not account for an ITF are characterized by an EUC that is dominated by northern component water. This is inconsistent with the ratio of northern to southern component water inferred from salinity measurements in the equatorial pycnocline. In our model runs, only when an ITF transport of between 10 and 20 Sv is imposed does the mixing ratio of northern to southern component waters come into accord with observations.

The strong sensitivity to the strength of the ITF was certainly an unexpected result. We have seen that the dynamical reason for this sensitivity can be understood by considering model flow fields within the pycnocline (shown in Figures 5c and 5d) for the cases with 0 and 10 Sv of ITF, respectively. The most significant impact of the changing the ITF transport occurs in the equatorward flowing LLWBCs of either hemisphere, namely, the Mindanao Current in the Northern Hemisphere, and the New Guinea Coastal Undercurrent (NGCUC) in the Southern Hemisphere. The equatorward transport of the Mindanao Current across 5°N at the western boundary is nearly the same for both model runs. However, with 0 Sv of ITF, nearly all of this northern component water directly feeds the equatorial undercurrent (EUC) upon reaching the equator, whereas with 10 Sv of ITF, much of the Mindanao Current water is diverted to the Indian Ocean. As for the inflow from the Southern Hemispheric LLWBC, the NGCUC is relatively weak with 0 Sv of ITF but is significantly strengthened for the case with 10 Sv of ITF, as seen in Figures 6c and 6d. It is principally the sensitivity of these LLWBCs to the strength of the imposed ITF transport that is reflected in the mixing ratio of our idealized tracers.

Given that this strong sensitivity exists, one would expect that the mixing ratio would be roughly 50/50 for the case with 0 Sv of ITF and dominated by the southern source for the case with 10 Sv of ITF. The point we wish to emphasize here is that the sensitivity exists but that it is not yet clear why the northern component is dominant for a closed Pacific domain. Our results are not inconsistent with those of *Lu and McCreary* [1995], since for all three cases (0, 10, and 20 Sv) an ITCZ "barrier" is maintained in the Northern Hemisphere. Lu and McCreary did not quantify a mixing ratio of northern to southern component water in their study, as their single passive tracer did not distinguish between northern and southern sources. It would be interesting to compare the results presented here with results obtained with other models such as theirs.

A meridional temperature gradient of amplitude 2°C exists on isopycnal surfaces in the western Pacific pycnocline, and thus changes in the mixing ratio of northern to southern component water have the potential to change the thermal structure of the pycnocline. Depending on the amplitude of these changes, this has the potential to change the thermal structure of the equatorial pycnocline and thus to influence climate. As has been shown with the CTD data collected along the repeat section at 165°E between 1984 and 1990, there is significant low-frequency variability in temperature and salinity within the pycnocline of the western equatorial Pacific. This is consistent with the recent findings of W.S. Kessler (personal communication, 1998), who has shown that low-frequency variability in the salinity structure of the western Pacific pycnocline accounts for as much as one third of the variance observed in dynamic height.

It remains to be determined whether the mechanism responsible for the observed subsurface temperature variability on isopycnals at 165°E is due to a mechanism of the type proposed by *Gu and Philander* [1997], by variability of the ITF transport as proposed in this study, by changes in diapycnal exchange rates, or by some combination thereof. The studies of *Gu and Philander* [1997] and *Blanke and Raynaud* [1997] have used point tracers to illustrate ventilation pathways for the Pacific thermocline circulation. Since these tracers only follow ventilation pathways determined by the model's advection equation, they are not influenced by the mix-

ing processes that occur within the model. However, we know from transient tracer measurements [*Quay et al.*, 1983] that such processes are not insignificant in the equatorial Pacific pycnocline.

As we have seen in Table 1, for our model runs, entrainment of cool water from below within the equatorial Pacific provides up to 25% of the water within the equatorial pycnocline for the cases where we account for the Indonesian Throughflow. Viewed in light of the model results of *Lu et al.* [1998], this could be less than the entrainment fluxes that occur in the real ocean, which might explain why the ITF transport required by our model is somewhat larger than the estimates from observations.

Future modeling work will involve forcing the model with seasonal and interannual winds and letting the model internally calculate its own ITF transport. This will allow us to address the magnitude of the effect of realistic ITF variability on the thermal budget of the equatorial pycnocline. Future model runs will also include tracers that facilitate quantification of diapycnal exchanges within the model.

Acknowledgments.
We would like to thank Arnold Gordon, Bill Jenkins, and Martin Visbeck for constructive comments and feedback. We would also like to thank John Toole at WHOI for making the CTD data at 165°E available to us. This work was supported by National Science Foundation contract numbers OCE-9633375 and OCE-9796253. This is Lamont-Doherty Earth Observatory contribution 5955.

References

Blanke, B., and S. Raynaud, Kinematics of the Pacific Equatorial Undercurrent: An Eulerian and Lagrangian approach from GCM results, *J. Phys. Oceanogr.*, *27*, 1038-1053, 1997.

Broecker, W.S., S. Sutherland, W. Smethie, T.-H. Peng, and G. Ostlund, Oceanic radiocarbon: separation of the natural and bomb components, *Global Biogeoch. Cycles*, *9*, 263-288, 1995.

Clement, A.C., R. Seager, M.A. Cane, and S.E. Zebiak, An ocean dynamical thermostat, *J. Clim.*, *9*, 2190-2196, 1996.

daSilva, A., C. Young, and S. Levitus, Atlas of surface marine data 1994, vol. 1, Algorithms and procedures, *NOAA Atlas NESDIS* 6, U.S. Dep. of Commer., Washington, D.C., 1994.

Deser, C., M.A. Alexander, and M.S. Timlin, Upper-ocean thermal variations in the North Pacific during 1970-1991, *J. Clim.*, *9*, 1840-1855, 1996.

Druffel, E., Radiocarbon in annual coral rings from the eastern tropical Pacific Ocean, *Geophys. Res. Lett.*, *8*, 59-62, 1981.

Druffel, E., Bomb radiocarbon in the Pacific, *J. Mar. Res.*, *19*, 35-46, 1987.

Ffield, A., and A.L. Gordon, Vertical mixing in the Indonesian thermocline, *J. Phys. Oceanogr.*, *22*, 184-195, 1992.

Fieux, M., C. Andrie, P. Delacluse, A.G. Ilahude, A. Kartavseff, F. Mantisi, R. Molcard, and J.C. Swallow, Measurements within the Pacific-Indian Oceans Throughflow region, *Deep Sea Res., Part 1*, *41*, 1091-1130, 1994.

Fieux, M., R. Molcard, and A.G. Ilahude, Geostrophic transport of the Pacific-Indian Oceans throughflow, *J. Geophys. Res.*, *101*, 12,421-12,432, 1996.

Fine, R.A., Direct evidence using Tritium data for throughflow from the Pacific into the Indian Ocean, *Nature*, *315*, 478-480, 1985.

Gent, P. R., and M. A. Cane, A reduced gravity, primitive equation model of the upper equatorial ocean, *J. Comput. Phys.*, *81*, 444-480, 1989.

Gent, P. R., and J. C. McWilliams, Isopycnal mixing in ocean circulation models, *J. Phys. Oceanogr.*, *20*, 150-155, 1990.

Gouriou, Y., and J. M. Toole, Mean circulation of the upper layers of the western equatorial Pacific Ocean, *J. Geophys. Res.*, *98*, 22,495-22,520, 1993.

Godfrey, J.S., A Sverdrup model of the depth-integrated flow for the World Ocean allowing for Island Circulations, *Geophys. Astrophys. Fluid Dyn.*, *45*, 89-112, 1989.

Godfrey, J.S., The effect of the Indonesian throughflow on ocean circulation and heat exchange with the atmosphere: A review, *J. Geophys. Res.*, *101*, 12,217-12,237, 1996.

Gordon, A.L., Interocean exchange of thermocline water, *J. Geophys. Res.*, *91*, 5037-5046, 1986.

Gordon, A.L., When is appearance reality? A comment on Why Does the Indonesian Throughflow Appear to Originate from the North Pacific, *J. Phys. Oceanogr.*, *25*, 1560-1570, 1995.

Griffies, S.M., The Gent-McWilliams skew-flux, *J. Phys. Oceanogr.*, *28*, 831-841, 1998.

Griffies, S.M., A. Gnanadesikan, R.C. Pacanowski, V.D. Larichev, J.K. Dukowicz, and R.D. Smith, Isoneutral diffusion in a z-coordinate ocean model, *J. Phys. Oceanogr.*, *28*, 805-830, 1998.

Gu, D., and S.G.H. Philander, Interdecadal climate fluctuations that depend on exchanges between the tropics and the extratropics, *Science*, *275*, 805-807, 1997.

Han, Y., A numerical world ocean general circulation model, II, A Baroclinic Experiment, *Dyn. Atmos. Oceans*, *8*, 141-172, 1984.

Hellerman, S., and M. Rosenstein, Normal monthly wind stress over the World Ocean with error estimates, *J. Phys. Oceanogr.*, *13*, 1093-1104, 1983.

Hirst, A. C., and J. S. Godfrey, The role of Indonesian throughflow in a global Ocean GCM, *J. Phys. Oceanogr.*, *23*, 1057-1086, 1993.

Jenkins, W.J., The exchange and upwelling of subtropical waters in the Tropical Pacific (abstract), *EOS Trans AGU*, *77*(46), Fall Meet. Suppl., 359, 1996.

Levitus, S., R. Burgett, and T. P. Boyer, *World Ocean Atlas 1994*, vol. 3, *Salinity*, 99 pp., U.S. Dep. of Commer., Washington, D. C., 1994.

Levitus, S., and T. P. Boyer, *World Ocean Atlas 1994*, vol. 4, *Temperature*, 117 pp., U.S. Dep. of Commer., Washington, D. C., 1994.

Liu, Z., and B. Huang, Why is there a tritium maximum in the Central Equatorial Pacific thermocline?, *J. Phys. Oceanogr.*, *28*, 1527-1533, 1998.

Liu, Z., and S. G. H. Philander, How different wind stress patterns affect the tropical-subtropical circulations in the upper ocean, *J. Phys. Oceanogr.*, *25*, 449-462, 1995.

Liu, Z., S. G. H. Philander, and R. C. Pacanowski, A GCM study of tropical-subtropical upper-ocean water exchange, *J. Phys. Oceanogr.*, *24*, 2606-2623, 1994.

Lu, P., and J.P. McCreary, Influence of the ITCZ on the flow of thermocline water from the subtropical to the Equatorial Pacific Ocean, *J. Phys. Oceanogr.*, *25*, 3076-3088, 1995.

Lu, P., J.P. McCreary, and B.A. Klinger, Meridional circulation cells and the source waters of the Pacific Equatorial Undercurrent, *J. Phys. Oceanogr.*, *28*, 62-84, 1998.

McCreary, J.P., and P. Lu, Interaction between the subtrop-

ical and the equatorial ocean circulations: The subtropical cell, *J. Phys. Oceanogr.*, *24*, 466-497, 1994.

Murray, S.P., S.P., E. Lindstrom, J. Kindle, and E. Weeks, Transport through Vitiaz Strait, *WOCE Notes*, *7*(1), 21-23, 1995.

Naik, N., M. A. Cane, S. Basin, and M. Israeli, A solver for the barotropic mode in the presence of variable topography and islands, *Mon. Weather Rev.*, *123*, 817-832, 1995.

Pacanowski, R.C., and S.G. Philander, Parameterization of vertical mixing in numerical models of the tropical oceans, *J. Phys. Oceanogr.*, *11*, 1443-1531, 1981.

Quay, P.D., M. Stuiver, and W.S. Broecker, Upwelling rates for the Equatorial Pacific Ocean derived from the bomb ^{14}C distribution, *J. Mar. Res.*, *41*, 769-793, 1983.

Redi, M.H., Oceanic isopycnal mixing by coordinate rotation, *J. Phys. Oceanogr.*, *12*, 1154-1158, 1982.

Rothstein, L.M., R.H. Zhang, A.J. Busalacchi, and D. Chen, A numerical simulation of the mean water pathways in the subtropical and tropical Pacific Ocean, *J. Phys. Oceanogr.*, *28*, 322-343, 1998.

Seager, R., B. Blumenthal, and Y. Kushnir, An advective atmospheric mixed layer model for ocean modeling purposes: Global simulation of surface heat fluxes, *J. Clim.*, *8*, 1951-1964, 1995.

Shriver, J.F., and H.E. Hurlburt, The contribution of the global thermohaline circulation to the Pacific to Indian Ocean throughflow via Indonesia, *J. Geophys. Res.*, *102*, 5491-5511, 1997.

Toggweiler, J. R., K. Dixon, and W. S. Broecker, The Peru upwelling and the ventilation of the South Pacific thermocline, *J. Geophys. Res.*, *96*, 20,467-20,497, 1991.

Tsuchiya, M., R. Lukas, R. A. Fine, E. Firing, and E. Lindstrom, Source waters of the Pacific Equatorial Undercurrent, *Prog. Oceanogr.*, *23*, 101-147, 1989.

Warner, M., J. Bullister, D. Wisegarves, R. Gammon, and R. Weiss, Basin-wide distributions of chlorofluorocarbons CFC-11 and CFC-12 in the North Pacific: 1985-1989, *J. Geophys. Res.*, *101*, 22,525-22,542, 1996.

Wyrtki, K., An estimate of equatorial upwelling in the Pacific, *J. Phys. Oceanogr.*, *11*, 1205-1214, 1981.

Zebiak, S.E., and M.A. Cane, Natural climate variability in a coupled model, in *Workshop on Greenhouse-Gas-Induced Climate Change: A Critical Appraisal of Simulations and Observations*, edited by M.E. Schlesinger, pp. 457-470, Elsevier, New York, 1991.

Zhang, R.-H., L.M. Rothstein, and A.J. Busalacchi, Origin of upper-ocean warming and El Nino changes in the tropical Pacific Ocean, *Nature*, *391*, 879-883, 1998.

K.B. Rodgers, Max-Planck-Institut für Meteorologie, Bundesstrasse 55, D-20146 Hamburg, Germany. (e-mail: rodgers@dkrz.de)

M.A. Cane and N. Naik, Lamont-Doherty Earth Observatory, Columbia University, Palisades, NY, 10964. (e-mail: mcane@ldeo.columbia.edu and naomi@ldeo.columbia.edu)

D.P. Schrag, Department of Earth and Planetary Sciences, Harvard University, Cambridge, MA, 02138. (e-mail: schrag@eps.harvard.edu)

(Received April 6, 1998; revised November 4, 1998; accepted November 17, 1998.)